Supplementary Figures S1 – S10

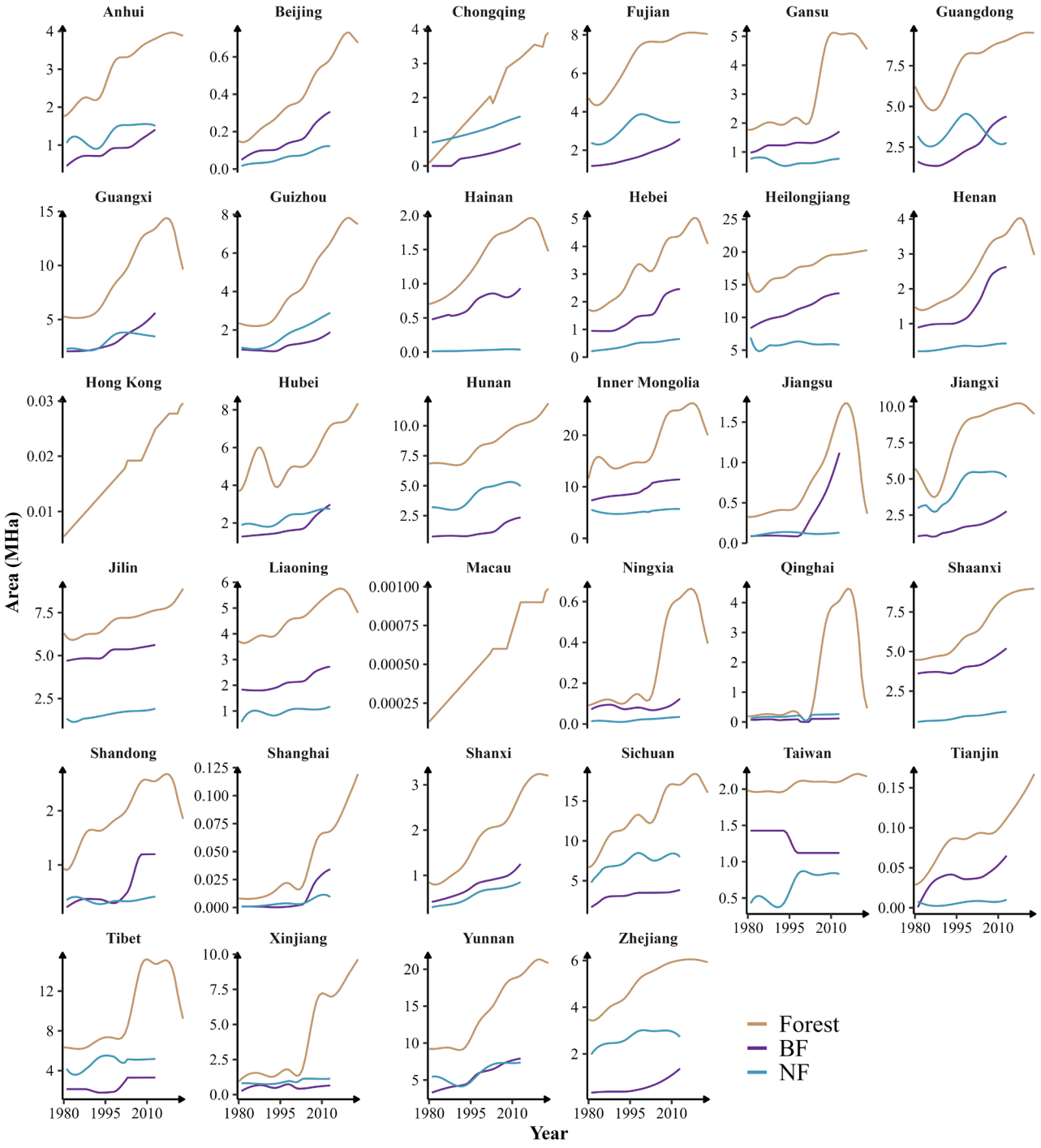

Figure S1. Time series of interpolated forest area for 34 provincial-level units from 1980 to 2023, showing total forest, needleleaf forest, and broadleaf forest areas derived from National Forest Inventory (NFI) data.

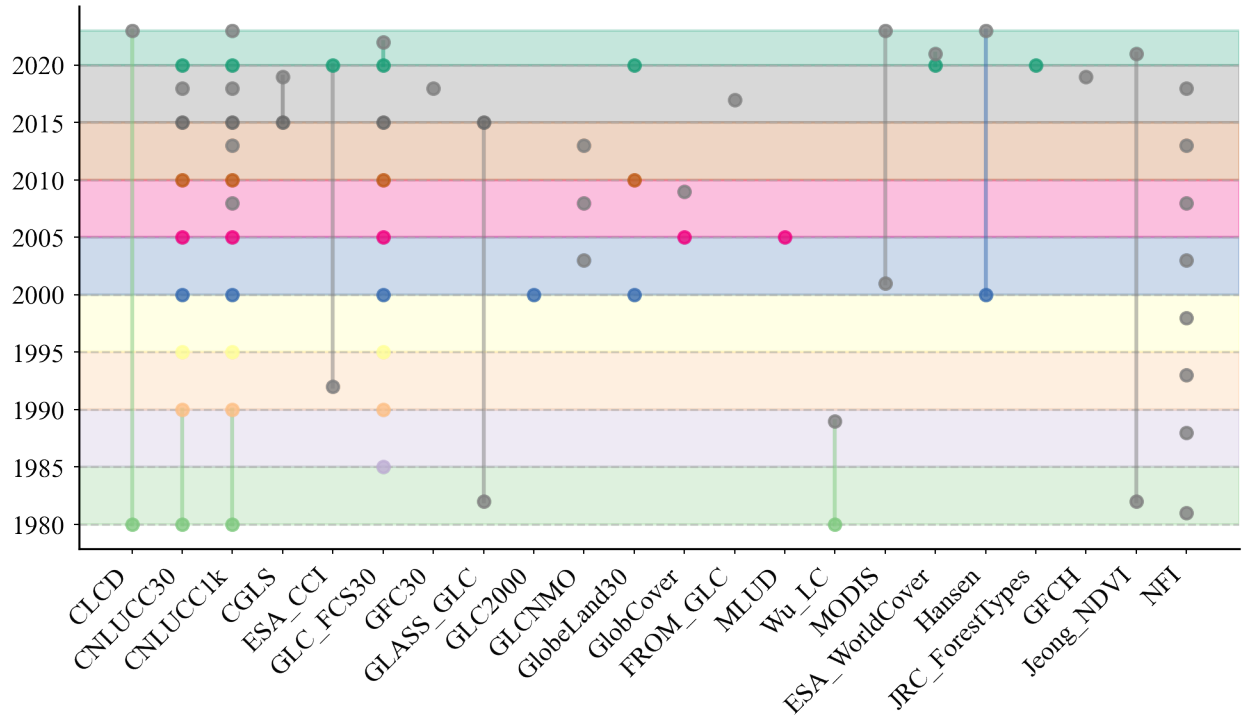

Figure S2. Schematic diagram illustrating the temporal coverage of the input datasets used for the forest reconstruction, including Land Use/Land Cover (LULC) products, NDVI data, and NFI survey periods.

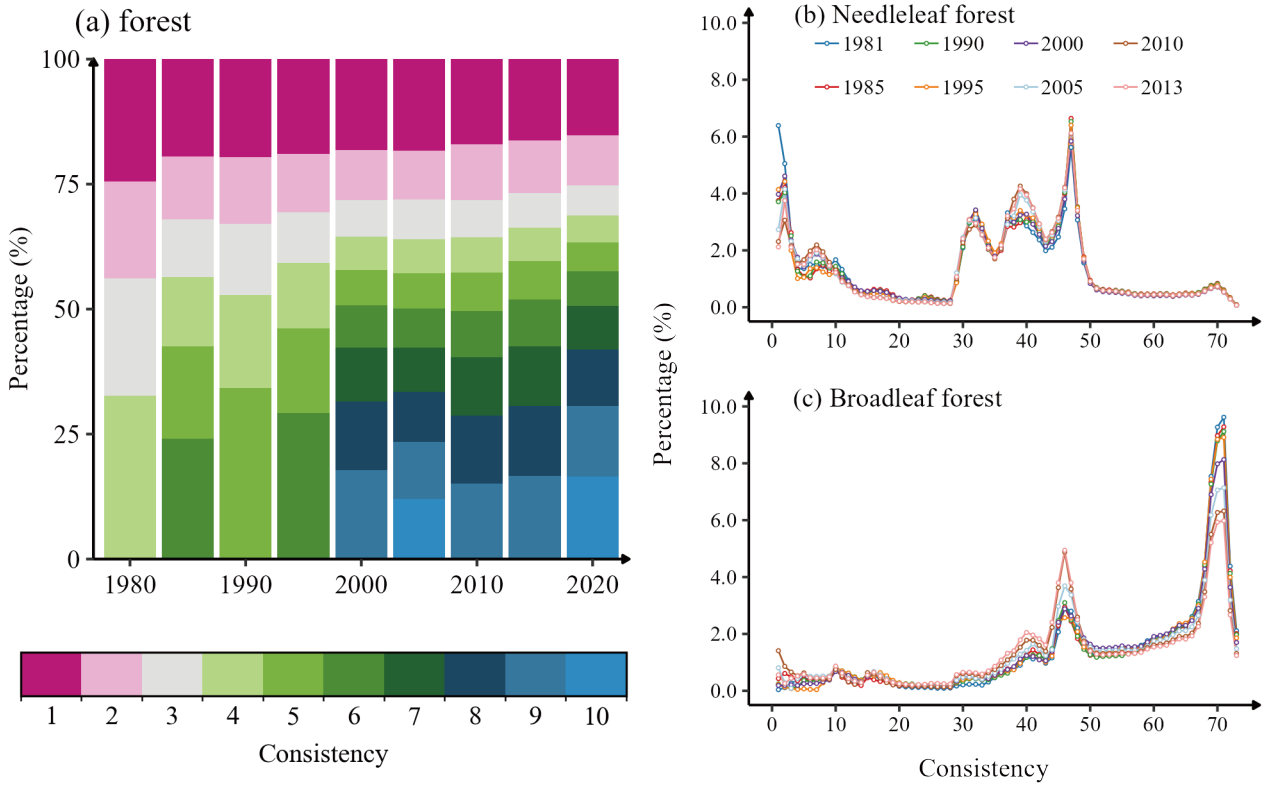

Figure S3. Inter-dataset consistency of forest cover in China. **(a)** Proportional distribution of potential forest pixels in China by consistency level for the years 1980, 1985, 1990, 1995, 2000, 2005, 2010, 2015, and 2020. The potential forest mask was generated annually by aggregating pixels classified as "forest" across all available LULC datasets. Consistency (***CON***) is defined as the number of datasets classifying a given pixel as forest; higher ***CON*** values therefore indicate greater inter-dataset agreement and a higher probability of a true forest classification. **(b, c)** Distribution of cross-dataset consistency scores for needleleaf and broadleaf forest classifications, respectively, for the period 1981–2013. These scores are derived from the Plant Functional Type (PFT) dataset reconstructed in this study, where higher scores signify greater confidence in the classifications for **(b)** needleleaf and **(c)** broadleaf.

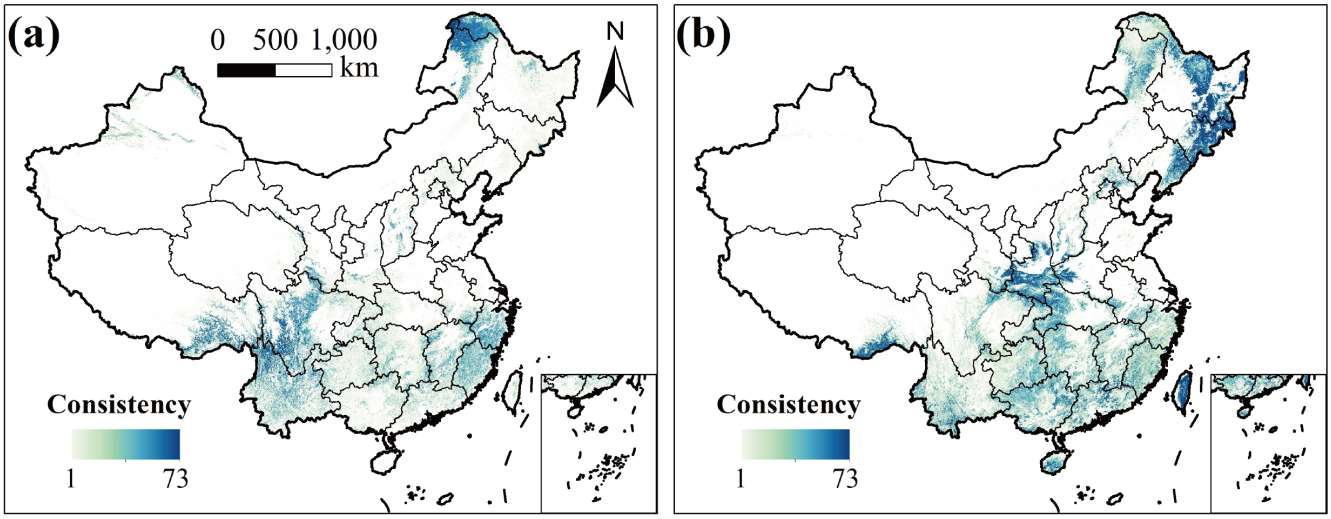

Figure S4. Static consistency maps for **(a)** needleleaf forests and **(b)** broadleaf forests, generated using all available LULC products from the 1980–2023 period.

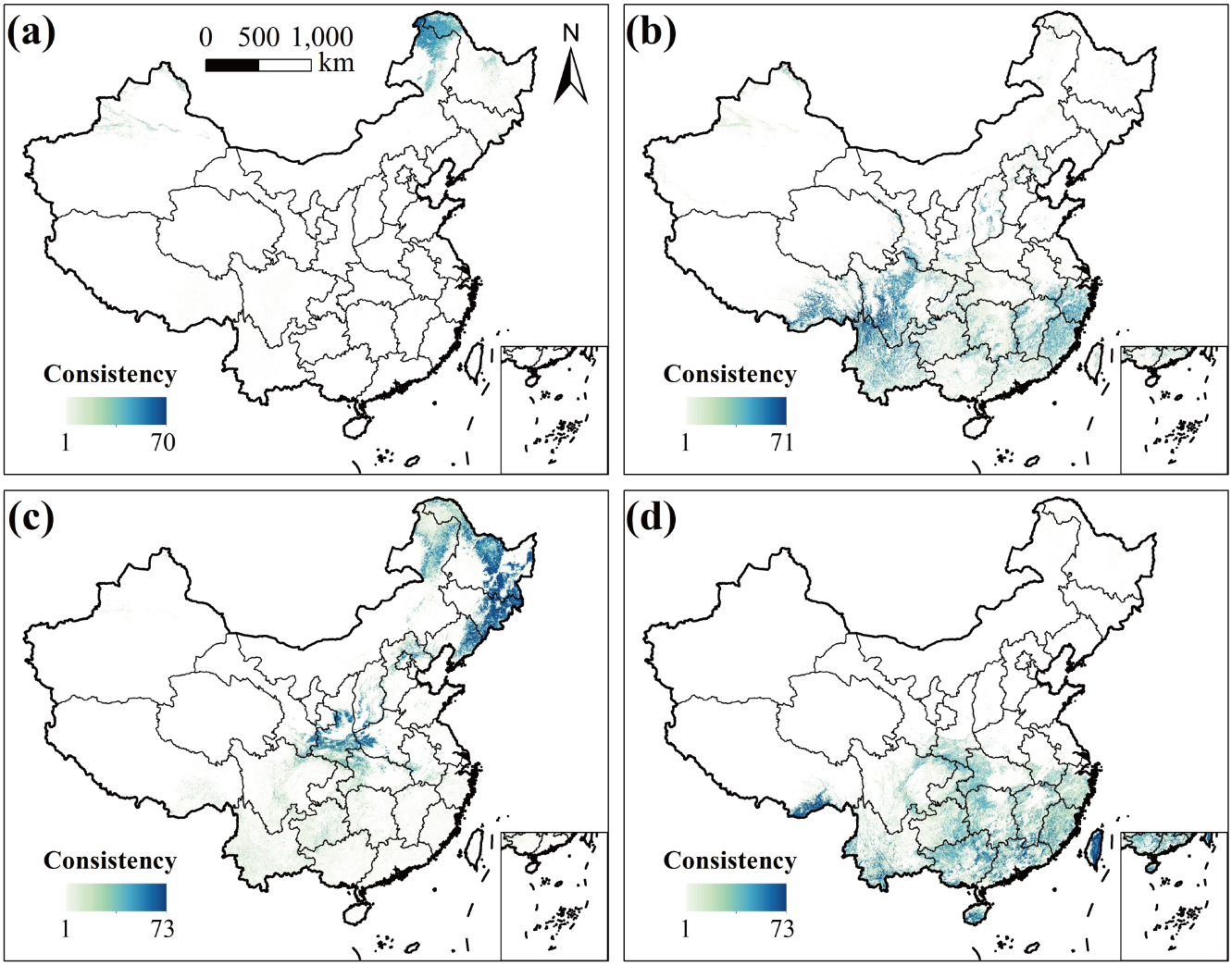

20 **Figure S5.** Static consistency maps for four phenological types, generated using all available data from the 1980–2023 period: **(a)** deciduous needleleaf, **(b)** evergreen needleleaf, **(c)** deciduous broadleaf, and **(d)** evergreen broadleaf forests.

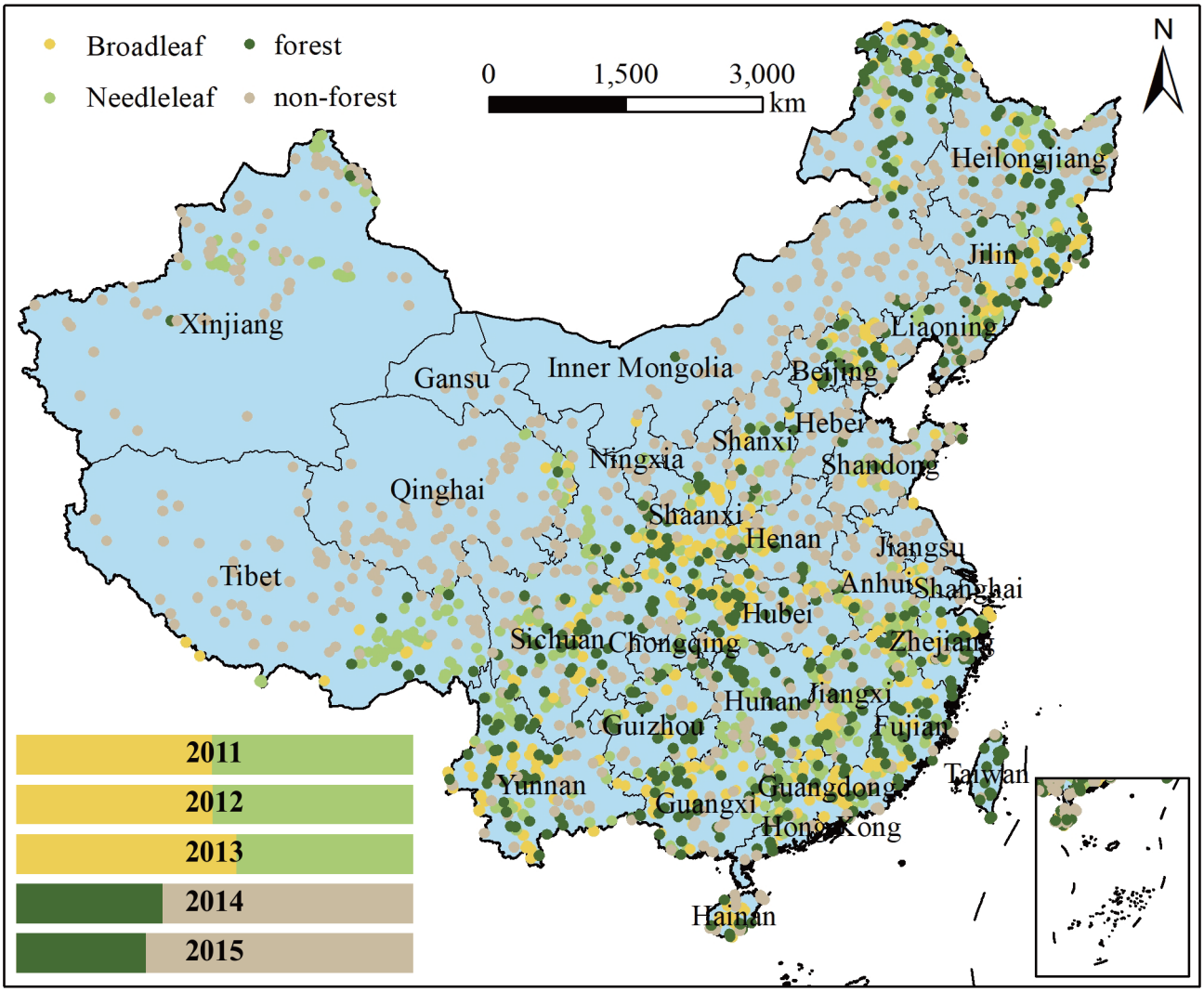

Figure S6. Spatial distribution of the independent forest validation sample points used for the accuracy assessment. The inset bar chart in the lower-left corner details the proportions of each land cover type.

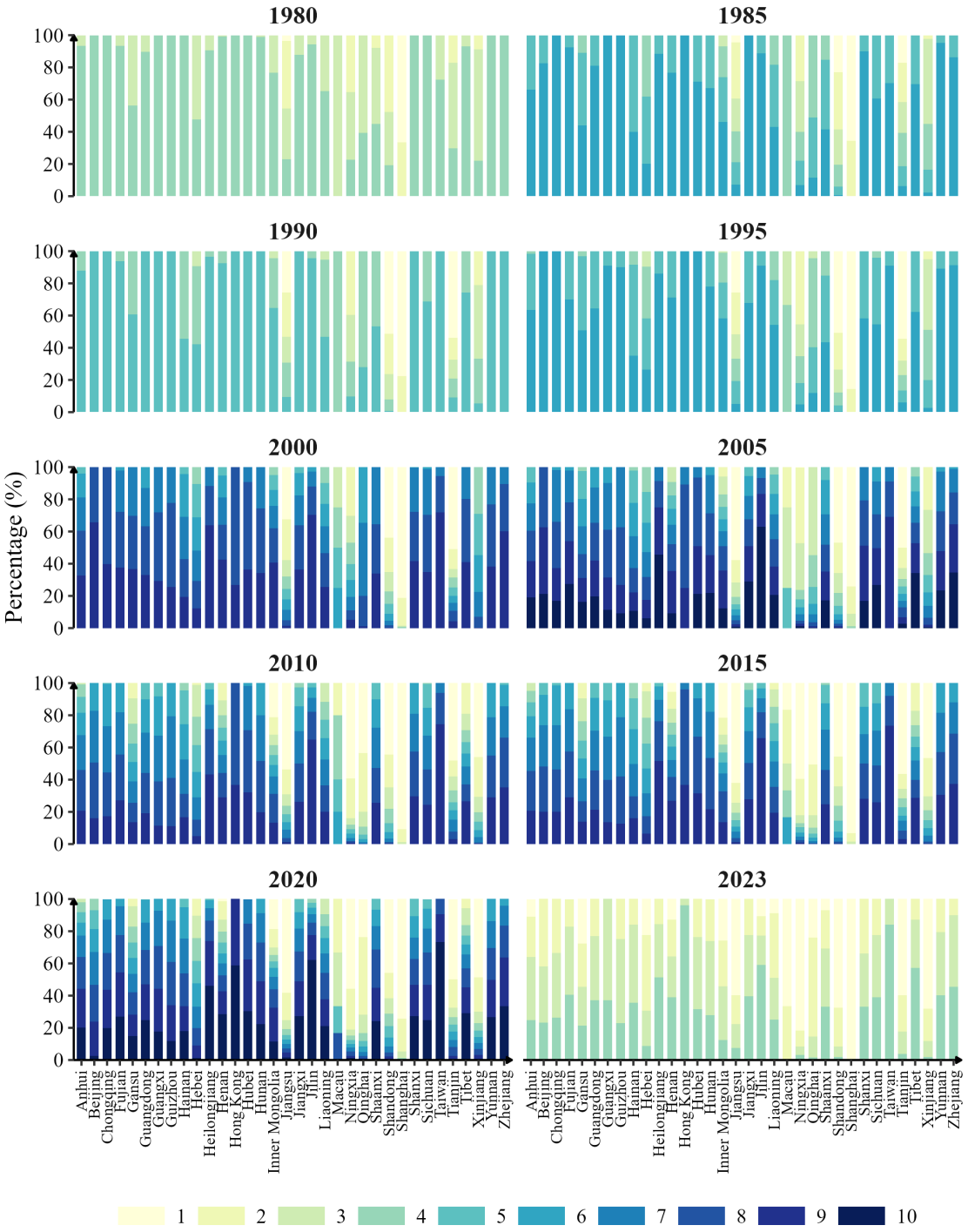

25

Figure S7. Provincial-level distribution of forest pixels according to their inter-dataset consistency score, assessed over the 1980-2023 period.

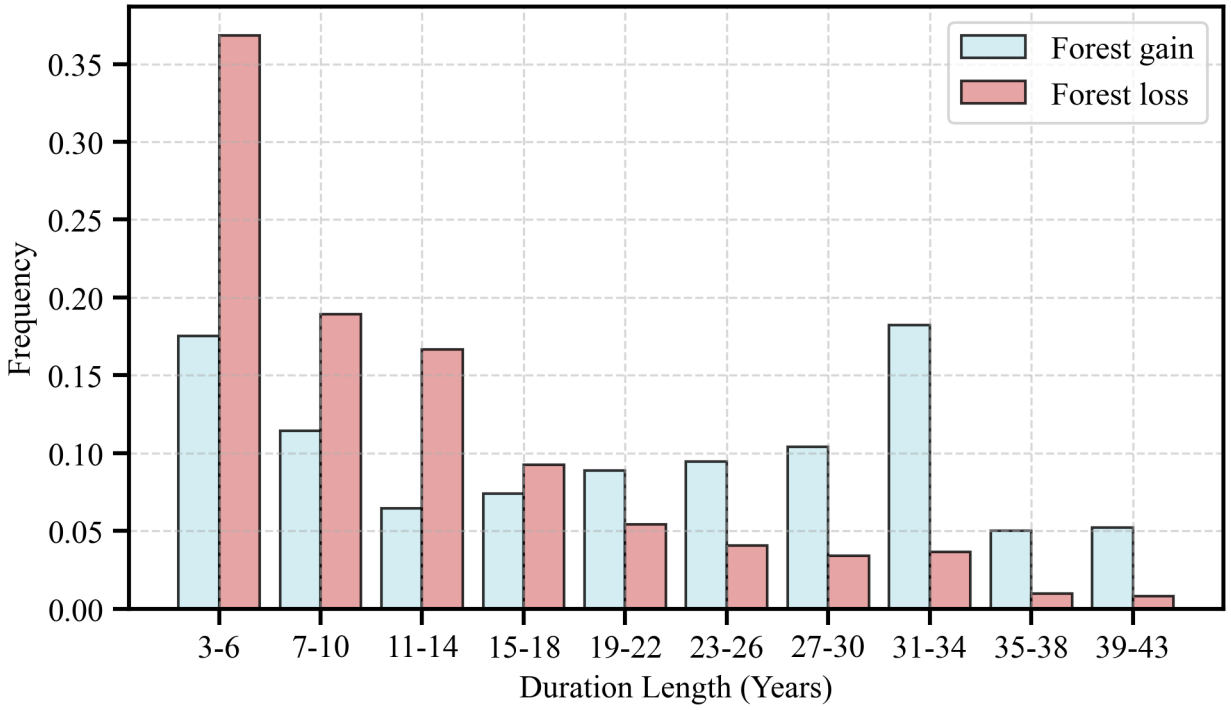

Figure S8. Frequency distribution histograms showing the duration of forest gain and loss events that occurred between 1980 and 2023

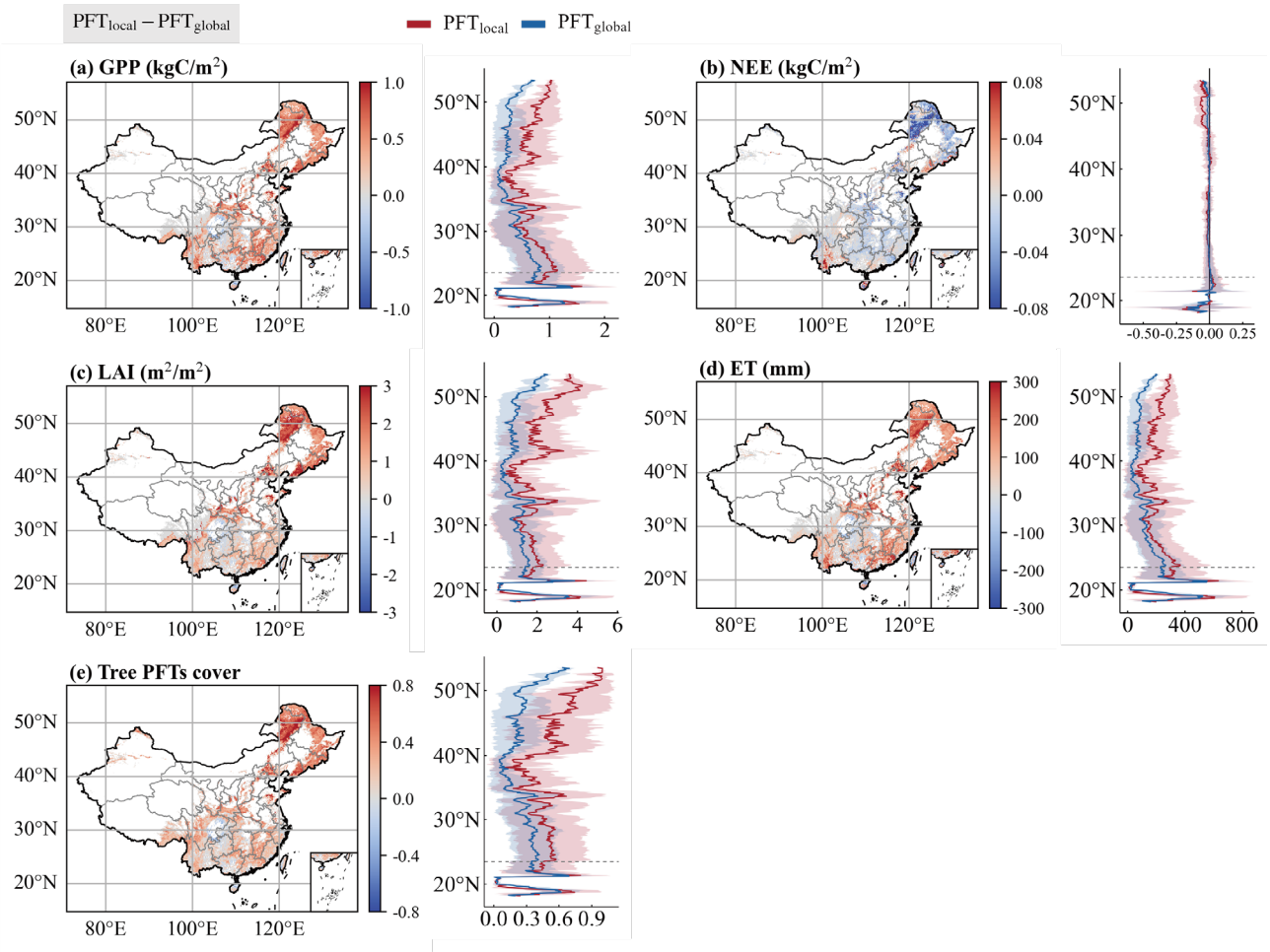

Figure S9. Comparison of Lund–Potsdam–Jena General Ecosystem Simulator (LPJ–GUESS) model simulations **(a–d)** and their underlying PFT forcing data **(e)** for the year 2010. The first four panels **(a–d)** show differences in simulated Gross Primary Productivity (GPP), Net Ecosystem Exchange (NEE), Leaf Area Index (LAI), and Actual Evapotranspiration (ET). Panel **(e)** shows differences in tree PFTs cover derived directly from the input PFT maps. For all panels, the maps display the spatial difference ($\boldsymbol{PFT_{local} - PFT_{global}}$), while the plots show the zonal mean and standard deviation for the $\boldsymbol{PFT_{local}}$ (red) and $\boldsymbol{PFT_{global}}$ (blue) datasets individually. Note that data in panels **(a-d)** are model outputs, whereas data in panel **(e)** are from the input maps.

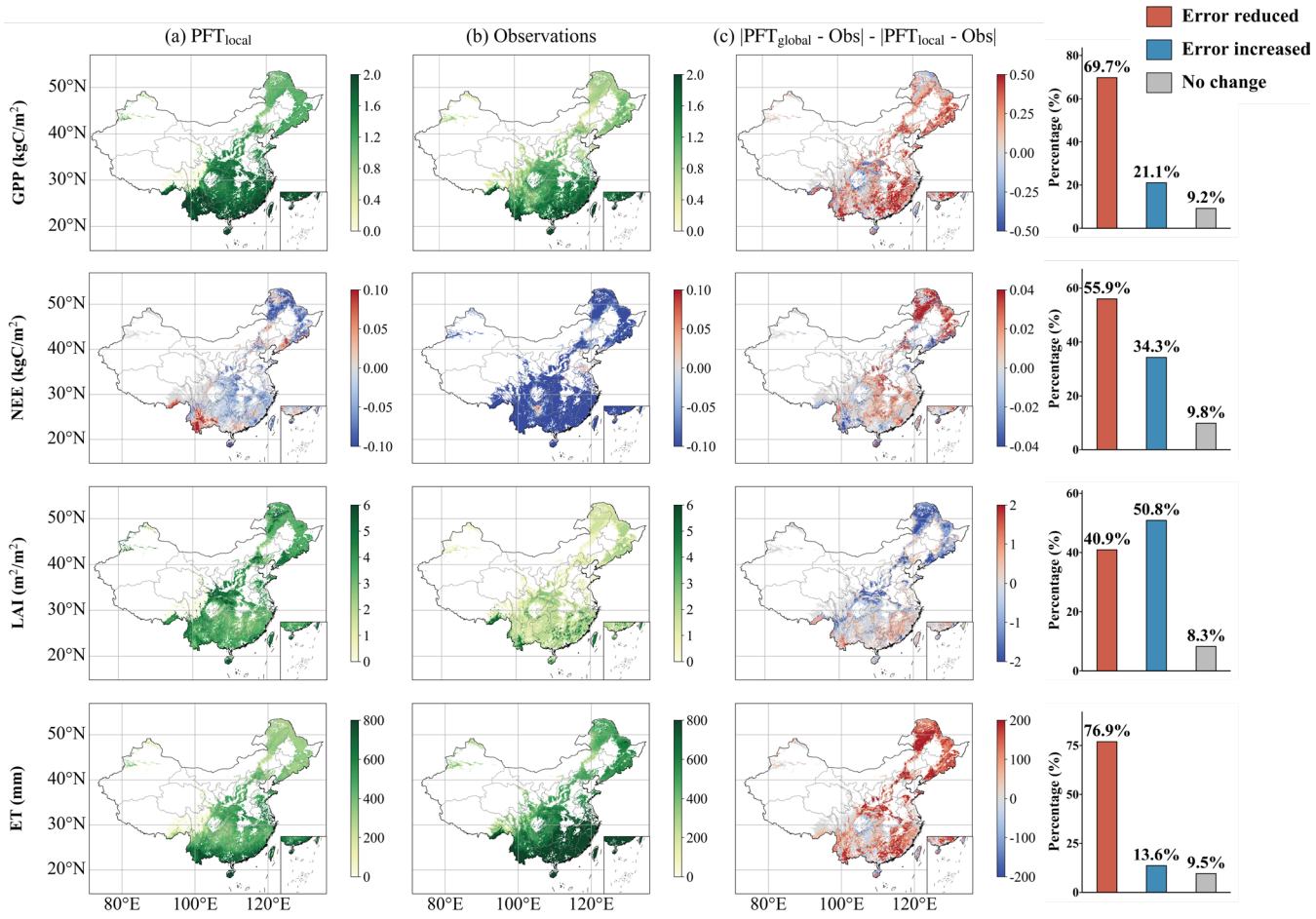

Figure S10. Annual model-data comparison for GPP, NEE, LAI, and ET for the year 2010. **(a)** Ecosystem variables simulated by the LPJ–GUESS model using our reconstructed $\boldsymbol{PFT_{local}}$ dataset. **(b)** Corresponding observation-based benchmark products from FLUXCOM (for GPP and NEE), GIMMS (for LAI4g), and GLEAM (for ET). **(c)** The difference in absolute error between model runs, calculated as $|\boldsymbol{PFT_{global}} - \boldsymbol{Observation}| - |\boldsymbol{PFT_{local}} - \boldsymbol{Observation}|$. Positive values indicate that $\boldsymbol{PFT_{local}}$ reduces the simulation error (improves performance) compared to $\boldsymbol{PFT_{global}}$, whereas negative values indicate an increase in error (performance degradation), and the right-hand bar graph displays the percentages of error reduced, increased, and no change.

Supplementary Tables S1 – S2

Table S1. LULC datasets used in this study.

Datasets	Resolution	Time range	Reference
CLCD[a,c]	30m	1980s-2023	(Yang and Huang, 2021)
CNLUCC[a,c]	1km	1980-2023	http://www.resdc.cn
CGLS[b,c]	100m	2015-2019	(Buchhorn et al., 2020)
ESA_CCI[b,c]	300m	1992-2020	https://data.ceda.ac.uk/neodc/esacci/land_cover/data
GLC_FCS30[b]	30m	1985-2022	(Zhang et al., 2020a)
GFC30[a]	30m	2018	(Zhang et al., 2020b)
GLASS_GLC[a,c]	5km	1982-2015	(Liu et al., 2020)
GLC2000[b]	1km	2000	(Bartholome and Belward, 2005)
GLCNMO[b]	1km	2003,2008,2013	(Tateishi et al., 2011)
GlobeLand30[a]	30m	2000,2010,2020	(Chen et al., 2015)
GlobCover[b]	300m	2005,2009	(Bontemps et al., 2011)
FROM_GLC[a]	10m	2017	(Gong et al., 2019)
MLUD[a]	250m	2005	(Ge et al., 2018)
Wu_LC[a]	1km	1980s	http://www.resdc.cn
MODIS[b,c]	500m	2001-2023	(Friedl et al., 2010)
ESA_WorldCover[a]	10m	2021,2022	https://esa-worldcover.org/en
Hansen[a]	30m	2000-2012	(Hansen et al., 2013)
JRC_ForestTypes[a]	10m	2020	(Bourgoin et al., 2025)
GFCH[a]	30m	2019	(Potapov et al., 2021)

[a.] These datasets delineate a single, general forest category and lack classification into specific subtypes.
[b.] These datasets provide detailed classifications of various forest subtypes.
[c.] These datasets are updated on an annual basis, in contrast to others which are produced only for specific years.

Table S2. Forest definition between NFI and LULC datasets.

Datasets	Forest Definition	Reference
NFI	Tree cover > 20%	http://www.forestdata.cn
CLCD	Tree cover > 15%	(Yang and Huang, 2021)
CNLUCC	Tree cover ≥ 10%	http://www.resdc.cn
CGLS	Tree cover > 15%	(Buchhorn et al., 2020)
ESA_CCI	Tree cover > 15%	https://data.ceda.ac.uk/neodc/esacci/land_cover/data
GLC_FCS30	Tree cover > 15%	(Zhang et al., 2020a)
GFC30	Tree cover > 10%, tree height > 5 m, land area > 0.5 ha	(Zhang et al., 2020b)
GLASS_GLC	Tree cover ≥ 10%; height > 5 m	(Liu et al., 2020)
GLC2000	Tree cover > 15%, height > 3 m	(Bartholome and Belward, 2005)
GLCNMO	Tree cover ≥ 10%	(Tateishi et al., 2011)
GlobeLand30	Tree cover > 10%	(Chen et al., 2015)
GlobCover	Tree cover > 15%, tree height > 5 m	(Bontemps et al., 2011)
FROM_GLC	Tree cover > 15%, tree height > 5 m	(Gong et al., 2019)
MLUD	Tree cover ≥ 10%	(Ge et al., 2018)
Wu_LC	Tree cover > 10%	http://www.resdc.cn
MODIS	Tree cover > 60%, tree height > 2 m	(Friedl et al., 2010)
ESA_WorldCover	Tree cover ≥ 10%	https://esa-worldcover.org/en
Hansen	Tree cover ≥ 50%, tree height > 5 m	(Hansen et al., 2013)
JRC_GFC2020	Tree cover > 10%, tree height > 5 m, land area > 0.5 ha	(Bourgoin et al., 2025)
GFCH	height ≥ 3 m	(Potapov et al., 2021)

References

Bartholomé, E., and Belward, A. S.: GLC2000: a new approach to global land cover mapping from Earth observation data, *Int. J. Remote Sens.*, 26, 1959–1977, https://doi.org/10.1080/01431160412331291297, 2005.

Bontemps, S., Defourny, P., Van Bogaert, E., Arino, O., Kalogirou, V., and Perez, J. J. R.: GLOBCOVER 2009 Products description and validation report, ESA, 2011.

Bourgoin, C., Verhegghen, A., Carboni, S., Degreve, L., Ameztoy Aramendi, I., Ceccherini, G., Colditz, R., and Achard, F.: Global forest maps for the year 2020 to support the EU regulation on deforestation-free supply chains, Publications Office of the European Union, Luxembourg, https://data.europa.eu/doi/10.2760/1975879, 2025.

Buchhorn, M., Lesiv, M., Tsendbazar, N.-E., Herold, M., Bertels, L., and Smets, B.: Copernicus global land cover layers—collection 2, *Remote Sens.*, 12, 1044, https://doi.org/10.3390/rs12061044, 2020.

Chen, J., Chen, J., Liao, A., Cao, X., Chen, L., Chen, X., He, C., Han, G., Peng, S., and Lu, M.: Global land cover mapping at 30 m resolution: A POK-based operational approach, *ISPRS J. Photogramm. Remote Sens.*, 103, 7–27, https://doi.org/10.1016/j.isprsjprs.2014.09.002, 2015.

Friedl, M. A., Sulla-Menashe, D., Tan, B., Schneider, A., Ramankutty, N., Sibley, A., and Huang, X.: MODIS Collection 5 global land cover: Algorithm refinements and characterization of new datasets, *Remote Sens. Environ.*, 114, 168–182, https://doi.org/10.1016/j.rse.2009.08.016, 2010.

Ge, Y., Jia, Y., Chen, Y., Xu, X., Jiang, D., and Zhang, D.: A multi-scale provincial land use dataset of the Chinese mainland based on super-resolution mapping, *J. Glob. Change Data Discov.*, 2, 323–330, https://doi.org/10.3974/geodp.2018.03.11, 2018.

Gong, P., Liu, H., Zhang, M., Li, C., Wang, J., Huang, H., Clinton, N., Ji, L., Li, W., Bai, Y., Chen, B., Xu, B., Zhu, Z., Yuan, C., Su, H. P., Guo, J., Xu, N., Li, W., Zhao, Y., Yang, J., Yu, C., Wang, X., Fu, H., Li, X., Li, W., Liu, C., Xu, F., Zhang, H., Chen, J., Feng, X., and Zhang, H.: Stable classification with limited sample: Transferring a 30-m resolution sample set collected in 2015 to mapping 10-m resolution global land cover in 2017, *Sci. Bull.*, 64, 370–373, https://doi.org/10.1016/j.scib.2019.03.002, 2019.

Hansen, M. C., Potapov, P. V., Moore, R., Hancher, M., Turubanova, S. A., Tyukavina, A., Thau, D., Stehman, S. V., Goetz, S. J., Loveland, T. R., Kommareddy, A., Egorov, A., Chini, L., Justice, C. O., and Townshend, J. R. G.: High-resolution global maps of 21st-century forest cover change, *Science*, 342, 850–853, https://doi.org/10.1126/science.1244693, 2013.

Liu, H., Gong, P., Wang, J., Clinton, N., Bai, Y., and Liang, S.: Annual dynamics of global land cover and its long-term changes from 1982 to 2015, *Earth Syst. Sci. Data*, 12, 1217–1243, https://doi.org/10.5194/essd-12-1217-2020, 2020.

Potapov, P., Li, X., Hernandez-Serna, A., Tyukavina, A., Hansen, M. C., Kommareddy, A., Pickens, A., Turubanova, S., Tang, H., Silva, C. E., Armston, J., Dubayah, R., Blair, J. B., and Hofton, M.: Mapping global forest canopy height through integration of GEDI and Landsat data, *Remote Sens. Environ.*, 253, 112165, https://doi.org/10.1016/j.rse.2020.112165, 2021.

Tateishi, R., Uriyangqai, B., Al-Bilbisi, H., Ghar, M. A., Tsend-Ayush, J., Kobayashi, T., Kasimu, A., Hoan, N. T., Shalaby, A., Alsaaideh, B., Enkhzaya, T., Gegentana, and Sato, H. P.: Production of global land cover data–GLCNMO, *Int. J. Digit. Earth*, 4, 22–49, https://doi.org/10.1080/17538941003777521, 2011.

Yang, J., and Huang, X.: 30 m annual land cover and its dynamics in China from 1990 to 2019, *Earth Syst. Sci. Data*, 13, 2021–2039, https://doi.org/10.5194/essd-13-2021-2021, 2021.

Zhang, X., Liu, L., Chen, X., Gao, Y., Xie, S., and Mi, J.: GLC_FCS30: Global land-cover product with fine classification system at 30 m using time-series Landsat imagery, *Earth Syst. Sci. Data*, 13, 2753–2776, https://doi.org/10.5194/essd-13-2753-2021, 2020a.

Zhang, X., Long, T., He, G., Guo, Y., Yin, R., Zhang, Z., Xiao, H., Li, M., and Cheng, B.: Rapid generation of global forest cover map using Landsat based on the forest ecological zones, *J. Appl. Remote Sens.*, 14, 022211, https://doi.org/10.1117/1.JRS.14.022211, 2020b.